Int. J. Heat Mass Transfer. Vol. 31, No. 9, pp. 1797–1806, 1988
Printed in Great Britain

0017-9310/88 $3.00+0.00

Analysis of periodically fully developed turbulent flow and heat transfer by k–ε equation model in artificially roughened annulus

B. K. LEE,† N. H. CHO‡ and Y. D. CHOI§

† Department of Industrial Safety Engineering, Choong Puk University, Chung Chu, Choong Puk, Korea
‡ Department of Mechanical Engineering, University of Sydney, N.S.W. 2006, Australia
§ Department of Mechanical Engineering, Korea University, Sung Puk, Seoul 136-701, Korea

(*Received* 6 *March* 1987 *and in final form* 14 *January* 1988)

Abstract—Periodic fully developed turbulent flows with heat transfer from an inner pipe in the artificially roughened annulus are analysed by the k–ε equation model. A new streamline curvature correction model of eddy viscosity and cyclic TDMA are applied in order to increase the accuracy and converging rate of numerical solutions. This paper illustrates the new method of obtaining the roughness functions from numerically predicted velocity and temperature profiles. A predicted roughness function related to the velocity profile agrees well with previous semi-empirical correlations, but that for the temperature profile shows a different shape from the previous ones.

1. INTRODUCTION

ARTIFICIAL roughness is made up of small ribs at regular intervals on the transfer surface, which act as turbulence promoters breaking up the viscous sublayer formed in the fluid region nearest to the wall. Since with artificial roughness, both heat transfer and friction losses increase, a study on the enhancement of heat transfer by artificial roughness should be performed along with a study on friction losses.

In the previous analyses on the variations of heat transfer and friction losses by artificial roughness, logarithmic laws of the wall

$$\bar{U}^+ = \frac{1}{\kappa}\ln\frac{y}{h} + R \tag{1}$$

$$\bar{T}^+ = \frac{Pr_t}{\kappa}\ln\frac{y}{h} + G \tag{2}$$

were used as the velocity and temperature profiles normal to the wall with roughness. Here R is the roughness function related to the velocity profile and G the roughness function related to the temperature profile.

Many transformation methods were proposed by Hall [1], Wilkie [2], Maubach [3], Dalle Donne and Meerwald [4], Dalle Donne and Meyer [5] and others to obtain R and G functions from experimental data for the friction and heat transfer in the artificially roughened annulus. Dalle Donne and Meyer [5], Han *et al.* [6] and Dipprey and Sabersky [7], and others proposed semi-empirical correlations for R and G as functions of h^+, P/H and Pr.

However, there are no universal correlations for R and G functions which can be applied to all the shapes of roughness and geometries of flow passage, because R and G functions vary not only with h^+, P/H and Pr, but also with shapes of roughness and geometries of flow passage. Therefore, in order to obtain the correlations of R and G for the new shape of roughness and geometry of flow passage, a lot of new experiments are necessary. Nevertheless, R and G functions cannot be obtained directly from the experimental data because they need complicated transformation processes which may cause the transformation errors since they use logarithmic laws of the wall which cannot correlate exactly the velocity and temperature in the region far from the wall.

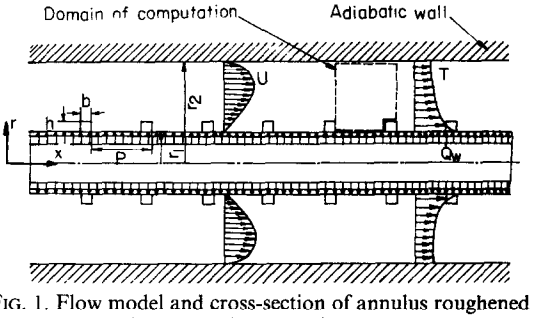

FIG. 1. Flow model and cross-section of annulus roughened by repeated rectangular ribs.

In this study a new method of obtaining R and G functions is illustrated. In this method, recirculating flows with heat transfer from the inner wall in the annulus with ring type rectangular roughness on the inner pipe as shown in Fig. 1 were analysed by the k–ε equation model. Functions R and G were calculated from predicted dimensionless velocity and temperature profiles. This method excludes the transformation errors which cannot be avoided in the previous methods. The only problem in this method is the accuracy of predictions of the velocity and temperature profiles.

Experimental studies reviewed in ref. [8] show that

NOMENCLATURE

C_μ, $C_{\mu 0}$, $C_{\varepsilon 1}$, σ_k, κ turbulence model constants
D_h hydraulic diameter [m]
G roughness function related to temperature profile
h, H height of roughness [m]
h^+ dimensionless height of roughness, $hU\tau/\nu$
k turbulent kinetic energy [$m^2 s^{-2}$]
L pitch of roughness [m]
P pitch of roughness [m], pressure [$N m^{-2}$]
Pe_t Peclet number
P_k production of turbulent kinetic energy [$kg m^{-1} s^{-3}$]
Pr Prandtl number
P_R periodic pressure [$N m^{-2}$]
Pr_t turbulent Prandtl number
Pr_{eff} effective Prandtl number
P_{ss}, P_{nn}, P_{ns} production of Reynolds stress in streamline coordinate [$kg m^{-1} s^{-3}$]
Q volume flow rate [$m^3 s^{-1}$]
Q_w wall heat flux [$W m^{-2}$]
Re Reynolds number, UDh/ν
r radial coordinate [m]
R radius of streamline curvature [m], radius of annulus [m], roughness function related to velocity profile
$\bar{T}^+$ dimensionless mean temperature
T_R periodic temperature [°C]
ΔT temperature rise in one pitch of roughness [°C]
U, V axial, radial velocity [$m s^{-1}$]
$\bar{U}^+$ dimensionless mean axial velocity
U_{ij} axial velocity at point (i, j) [$m s^{-1}$]
U_s, U_n, U_r s-, n-, r-direction velocity in streamline coordinate [$m s^{-1}$]
$\overline{u_n^2}$, $\overline{u_s^2}$, $\overline{u_n u_s}$ Reynolds stress in streamline coordinate [$m^2 s^{-2}$]
y distance from wall [m]
y^+ dimensionless distance from wall.

Greek symbols

β mean axial pressure gradient [$N m^{-3}$]
γ mean rate of temperature rise [$°C m^{-1}$]
λ friction factor
μ, μ_t, μ_{eff} viscosity, turbulent viscosity, effective viscosity [$kg m^{-1} s^{-1}$]
ν kinematic viscosity [$m^2 s^{-1}$]
ρ density [$kg m^{-3}$].

Subscripts

eff effective
k turbulent kinetic energy
n, s, r direction in streamline coordinate
R periodic
ref reference
t turbulence
w wall
1 inner wall
2 outer wall.

the turbulent shear stress and degree of anisotropy between normal stresses are very sensitive to streamline curvature. Several theoretical studies [9, 10] show that this sensitivity is not reflected by the standard k–ε model, and that modification of the k–ε model need to be introduced to achieve proper response. Leschziner and Rodi [11] derived theoretically the curvature correction equation for eddy viscosity from the algebraic stress equation of Reynolds stresses taken at the streamline coordinate system. Applying this correction of the k–ε model to the analysis of annular and twin parallel jets, they obtained greatly improved predictions compared with the standard k–ε model.

However, we have a different view from the derivation procedure of Leschziner and Rodi's model from the algebraic stress equation at the streamline coordinate system. In the present analysis, a new curvature correction equation was derived from the modified algebraic stress equations proposed by Launder [12], and it was applied to the analysis. Predictions of velocity and temperature profiles and pressure gradients by the modified curvature correction model agree well with experimental data. The predicted R function agrees reasonably well with previous correlations, however the G function has a different profile from previous ones.

In order to analyse the periodic fully developed flow with heat transfer in the annular pipe generally, momentum equations and energy equations should be integrated from the entrance to the region of fully developed velocity and temperature profiles. However, since they need a lot of computational work, in this analysis, a special method of calculation of the periodic fully developed flow proposed by Patankar *et al.* [13] was applied with some modifications of the converging scheme in order to increase the converging rate of the numerical solution.

2. GOVERNING EQUATION

As proposed by Patankar *et al.* [13], the pressure in periodic fully developed flows can be expressed as

$$P(x, r) = -\beta x + P_R(x, r) \tag{3}$$

where β is a mean pressure gradient and $P_R(x, r)$ behaves in a periodic fashion from module to module. The term βx is indicative of the general pressure drop that takes place in the flow direction. Since the fluid temperature T would, in general, rise in the flow direc-

tion, it does not behave in a periodic fashion. It is therefore convenient to express T as

$$T(x,r) = \gamma x + T_R(x,r) \tag{4}$$

where $\gamma = \Delta T/L$, then $T_R(x,r)$ would vary periodically from module to module.

The governing equations can now be written as:

continuity

$$\frac{\partial}{\partial x}(\rho U) + \frac{1}{r}\frac{\partial}{\partial r}(r\rho V) = 0; \tag{5}$$

x-momentum

$$\frac{\partial}{\partial x}(\rho UU) + \frac{1}{r}\frac{\partial}{\partial r}(r\rho VU) = -\frac{\partial P_R}{\partial x} + \frac{\partial}{\partial x}\left(\mu_{\text{eff}}\left(2\frac{\partial U}{\partial x}\right)\right) + \beta + \frac{1}{r}\frac{\partial}{\partial r}\left(r\mu_{\text{eff}}\left(\frac{\partial V}{\partial x} + \frac{\partial U}{\partial r}\right)\right) - \frac{2}{3}\frac{\partial(\rho k)}{\partial x}; \tag{6}$$

r-momentum

$$\frac{\partial}{\partial x}(\rho UV) + \frac{1}{r}\frac{\partial}{\partial r}(r\rho VV) = -\frac{\partial P_R}{\partial r} + \frac{\partial}{\partial x}\left(\mu_{\text{eff}}\left(\frac{\partial V}{\partial x} + \frac{\partial U}{\partial r}\right)\right) + \frac{1}{r}\frac{\partial}{\partial r}\left(r\mu_{\text{eff}}\left(2\frac{\partial V}{\partial r}\right)\right) - 2\mu_{\text{eff}}\frac{V}{r^2} - \frac{2}{3}\frac{\partial(\rho k)}{\partial r}; \tag{7}$$

thermal energy

$$\frac{\partial}{\partial x}(\rho UT_R) + \frac{1}{r}\frac{\partial}{\partial r}(r\rho VT_R) = \frac{\partial}{\partial x}\left(\frac{\mu_{\text{eff}}}{Pr_{\text{eff}}}\frac{\partial T_R}{\partial x}\right) + \frac{1}{r}\frac{\partial}{\partial r}\left(r\frac{\mu_{\text{eff}}}{Pr_{\text{eff}}}\frac{\partial T_R}{\partial r}\right) - \rho U\gamma; \tag{8}$$

turbulent kinetic energy

$$\frac{\partial}{\partial x}(\rho Uk) + \frac{1}{r}\frac{\partial}{\partial r}(r\rho Vk) = \frac{\partial}{\partial x}\left(\frac{\mu_{\text{eff}}}{\sigma_k}\frac{\partial k}{\partial x}\right) + \frac{1}{r}\frac{\partial}{\partial r}\left(r\frac{\mu_{\text{eff}}}{\sigma_k}\frac{\partial k}{\partial r}\right) + P_k - \rho\varepsilon; \tag{9}$$

dissipation rate of turbulent kinetic energy

$$\frac{\partial}{\partial x}(\rho U\varepsilon) + \frac{1}{r}\frac{\partial}{\partial r}(r\rho V\varepsilon) = \frac{\partial}{\partial x}\left(\frac{\mu_{\text{eff}}}{\sigma_\varepsilon}\frac{\partial \varepsilon}{\partial x}\right) + \frac{1}{r}\frac{\partial}{\partial r}\left(r\frac{\mu_{\text{eff}}}{\sigma_\varepsilon}\frac{\partial \varepsilon}{\partial r}\right) + C_{\varepsilon 1}\frac{\varepsilon}{k}P_k - C_{\varepsilon 2}\frac{\varepsilon^2}{k} \tag{10}$$

Table 1. Values of turbulent model constants

C_μ	$C_{\varepsilon 1}$	$C_{\varepsilon 2}$	σ_k	σ_ε	κ
0.09	1.44	1.92	1.0	$\dfrac{\kappa^2}{(C_{\varepsilon 2}-C_{\varepsilon 1})C_\mu^{1/2}}$	0.4187

where

$$P_k = \mu_t\left(2\left(\left(\frac{\partial U}{\partial x}\right)^2 + \left(\frac{\partial V}{\partial r}\right)^2 + \left(\frac{V}{r}\right)^2\right) + \left(\frac{\partial V}{\partial x} + \frac{\partial U}{\partial r}\right)^2\right). \tag{11}$$

Turbulent viscosity is related to k and ε by

$$\mu_t = C_\mu \rho \frac{k^2}{\varepsilon}. \tag{12}$$

The constants appearing in equations (10)–(12) take values in Table 1 which are taken from Launder *et al.* [14].

2.1. *Streamline curvature correction*

Turbulence in the shear layer is highly sensitive to streamline curvature in the plane of the mean shear. Several theoretical studies [9, 10] show that this sensitivity is not reflected by the standard k–ε model, and that a modification needs to be introduced to achieve proper response. In the present analysis, three kinds of streamline curvature correction models were examined; HL model [15], LPS model [9], LR model [11]. Of these, the third has reduced most the discrepancies between the predicted velocity profiles and pressure gradients of the experimental data of refs. [16–18].

However, we have a different view from the derivation procedure of Leschziner and Rodi's model from the algebraic stress equation taken in the streamline coordinate system. They used the production of Reynolds stresses as follows:

$$P_{ss} = -2\overline{u_s^2}\frac{\partial U_s}{\partial s} - 2\overline{u_s u_n}\left(\frac{\partial U_s}{\partial n} + \frac{U_s}{R}\right) \tag{13}$$

$$P_{nn} = -2\overline{u_n^2}\frac{\partial U_n}{\partial n} + 4\overline{u_n u_s}\frac{U_s}{R} \tag{14}$$

$$P_{ns} = -\overline{u_n^2}\frac{\partial U_s}{\partial n} + (2\overline{u_s^2} - \overline{u_n^2})\frac{U_s}{R} + \overline{u_n u_s}\frac{U_r}{R} \tag{15}$$

where s is the streamline direction and n the direction normal to the streamline as shown in Fig. 2.

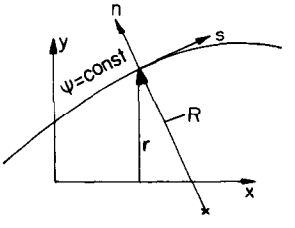

FIG. 2. Streamline coordinate system.

From the above equations they derive the following curvature correction equation for C_μ:

$$C_\mu = \frac{C_{\mu 0}}{1+8K_1^2\frac{k^2}{\varepsilon^2}\left(\frac{\partial U_s}{\partial n}+\frac{U_s}{R}\right)\frac{U_s}{R}} \tag{16}$$

where $K_1 = 0.267$, $C_{\mu 0} = 0.09$.

However, Launder [12] proposed that it is more reasonable that the production of Reynolds stresses in the streamline coordinate be derived by the coordinate transformation procedure of Aris from the Cartesian coordinate [20].

If production of Reynolds stresses was derived by the transformation procedure of Aris, it would be as follows [21]:

$$P_{ss} = -2\overline{u_s^2}\frac{\partial U_s}{\partial s} - 2\overline{u_s u_n}\frac{\partial U_s}{\partial n} - 2\frac{U_r}{R}\overline{u_s^2} \tag{17}$$

$$P_{nn} = -2\overline{u_n^2}\frac{\partial U_n}{\partial n} + 2\overline{u_n u_s}\frac{U_s}{R} \tag{18}$$

$$P_{ns} = -\overline{u_n^2}\frac{\partial U_s}{\partial n} + \overline{u_s^2}\frac{U_s}{R} - \overline{u_n u_s}\frac{U_r}{R}. \tag{19}$$

With equations (17)–(19), we could derive the following modified curvature correction equation of the LR model

$$C_\mu = \frac{C_{\mu 0}}{1+4K_1^2\frac{k^2}{\varepsilon^2}\frac{\partial U_s}{\partial n}\frac{U_s}{R}}. \tag{20}$$

In this study the modified curvature correction model was examined and it was found that the predictions by this model agreed well with experimental data and gave better convergence of solutions than the LR model.

3. NUMERICAL ANALYSIS

Finite difference equations were solved by the SIMPLER scheme proposed by Patankar [22]. This study examined the performance of two discretization schemes for convection for the standard k–ε model solutions.

(1) Hybrid differencing scheme (HDS).

(2) Quadratic upstream weighted interpolation for convective kinematics (QUICK).

The QUICK scheme was proposed by Leonard [23] as the method to minimize the numerical diffusion. When the curvature correction model was used, only the QUICK scheme was employed for the discretization scheme.

3.1. *Numerical analysis of momentum equation*

In order to solve equation (6) for a given Re, β should be known. Patankar and co-workers [13, 24] set β equal to a convenient constant value (e.g. $\beta = 1$) in the analysis of periodic fully developed laminar flow. Iterations for solving the flow equations were performed with a tentative value of fluid viscosity μ. Then the resulting velocity field was used to calculate average velocity. The viscosity μ was then recalculated such that the value of the average velocity implied the given Re.

However, in the analysis of turbulent flow this method cannot be used since turbulent viscosity is not uniform all over the flow region. Therefore, in this analysis a new method was suggested. First β is assumed to be

$$\beta = \frac{p(x,r)-p(x+L,r)}{L} = \lambda\frac{\rho v^2 Re}{2D_h^2} \tag{21}$$

where L is the length of one pitch of roughness and λ the friction factor. Then iterations for calculation of momentum equations were performed. The flow rate (Q) is calculated from the resulting velocity field and β was corrected by the following equation:

$$\beta_{new} = \beta_{old}\left(1+\alpha\left(\left(\frac{Q_0}{Q}\right)^2-1\right)\right) \tag{22}$$

where Q_0 is the flow rate for a given Re, β_{old} is the value of β of the previous iteration and α is the over-relaxation factor. A number of tests showed that $\alpha = 30$–40 lead to the fastest converging rate of solutions. In order to facilitate the converging rate of solution, alternating sweeps of cyclic TDMA in the r-direction and normal TDMA in the x-direction were applied.

3.2. *Computational details and boundary conditions*

Computations here were performed with meshes varying from 18×25 to 33×40 non-uniformly distributed grid lines according to the Reynolds number and P/H. Fine grids were located in the regions near the walls. We tested the effect of a number of grids on the computational results. The results for QUICK with the present number of grids are probably accurate enough to be regarded as grid-independent solutions.

Boundary conditions used for the present computations are summarized in Table 2. Table 2 shows that inlet conditions are given by outlet conditions and outlet conditions by inlet conditions. Therefore, in order for the solution to be converged, not only residual sources of finite difference equations, but also β should be converged. In this analysis the following strict converging criterion of β was used:

$$\left|\frac{\beta_{new}-\beta_{old}}{\beta_{old}}\right| \leqslant 10^{-5}. \tag{23}$$

4. COMPUTATIONAL RESULTS AND DISCUSSION

Computations were performed for the annulus with a radius ratio (R_1/R_2) of 0.392, ratio of roughness height to hydraulic diameter of annulus (H/D_h) of

Table 2. Summary of boundary conditions

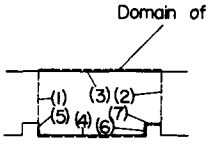

	U	V	P_R	P'	k	ε	T_R
(1) Inlet	U_{outlet}	V_{outlet}	$P_{R\,outlet}$	P'_{outlet}	k_{outlet}	ε_{outlet}	$T_{R\,outlet}$
(2) Outlet	U_{inlet}	V_{inlet}	$P_{R\,inlet}$	P'_{inlet}	k_{inlet}	ε_{inlet}	$T_{R\,inlet}$
(3) Outer wall	$U_B = 0$ W.F.	$V_n = 0$	$A_n = 0$	W.F.	W.F.	W.F.	Adiabatic ($dT_R/dr = 0$)
(4) Inner wall	$U_B = 0$	$V_s = 0$	$A_s = 0$	$A_s = 0$	W.F.	W.F.	Constant heat flux
(5) Front roughness vertical wall	$U_w = 0$	$V_B = 0$ W.F.	$A_w = 0$	$A_w = 0$	W.F.	W.F.	Constant heat flux
(6) Rear roughness vertical wall	$U_e = 0$	$V_B = 0$ W.F.	$A_e = 0$	$A_e = 0$	W.F.	W.F.	Constant heat flux
(7) Roughness upper wall	$U_B = 0$ W.F.	$V_s = 0$	$A_s = 0$	$A_s = 0$	W.F.	W.F.	Constant heat flux

0.0506, and ratio of pitch to height of roughness (P/H) of 3–20. In the following, selected computational results are presented and compared with experimental data [16–19].

Figure 3 compares velocity distributions predicted by the QUICK and HYBRID schemes at the standard k–ε model for $P/H = 20$ and $Re = 39\,000$. There are little differences in velocity profiles in the core region and outer wall layer. This is due to the fact that in these regions streamlines are nearly parallel to grid lines, so little numerical diffusion takes place. However, in the recirculating flow region near the roughness, differences of velocities are significant. This may be caused by the increase of numerical diffusion at the HYBRID scheme due to the inclined intersection of streamlines and grid lines.

Both QUICK and HYBRID solutions agree well with Kang's [16] experimental data in the core region, however, approaching the outer and inner wall, discrepancies increase.

Figures 4 and 5 compare the velocity distributions predicted by the standard k–ε model with the present curvature correction model. Velocity profiles of the present curvature correction model agree better with Kang's data except near the bottom wall where experimental errors are large due to the backward velocity. For other values of P/H and Reynolds numbers, the present curvature correction model also gives the best velocity profiles of all the results from the models examined in this study.

Turbulent kinetic energy profiles predicted by the present curvature correction model for $Re = 30\,000$ and $P/H = 15$ are shown in Fig. 6. It shows that turbulent kinetic energy is produced by the ribs and has a maximum value just in front of the ribs.

The ratio of the production rate of turbulent kinetic energy to the dissipation rate of turbulent kinetic energy is shown in Fig. 7. It shows that the production rate and the dissipation rate are nearly in equilibrium

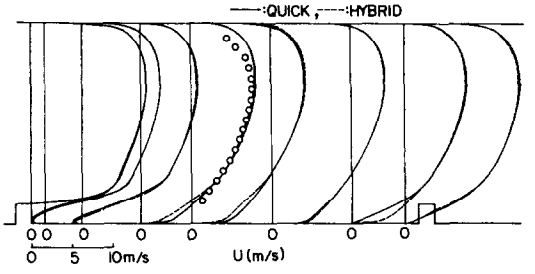

FIG. 3. Axial velocity profiles for $Re = 39\,000$ and $P/H = 20$. Data were taken from Kang [16].

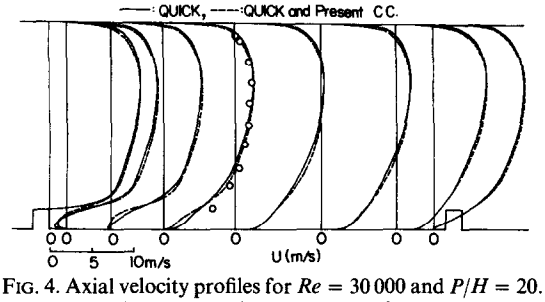

FIG. 4. Axial velocity profiles for $Re = 30\,000$ and $P/H = 20$. Data were taken from Kang [16].

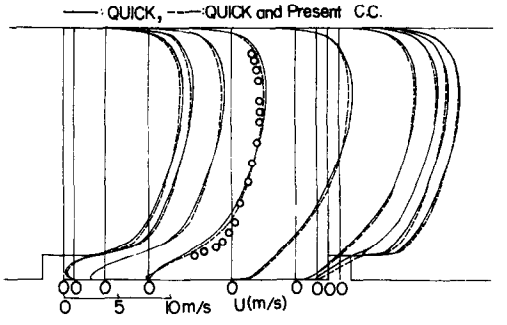

FIG. 5. Axial velocity profiles for $Re = 30\,000$ and $P/H = 10.8$. Data were taken from Kang [16].

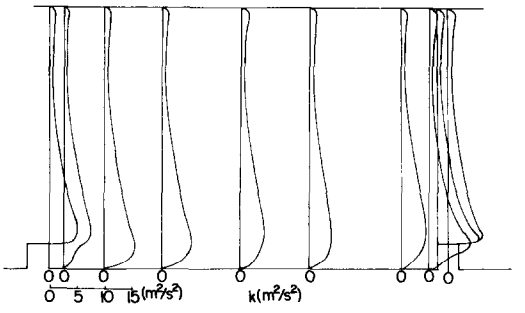

FIG. 6. Turbulent kinetic energy profiles for $Re = 30\,000$ and $P/H = 15$.

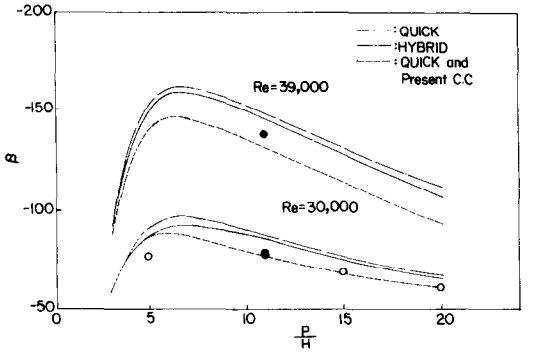

FIG. 8. Mean axial pressure gradient with respect to P/H: ○, ref. [19] semi-empirical prediction; ●, ref. [18] experiment.

near the outer wall, but in the other regions they are not in equilibrium.

Figure 8 compares mean axial pressure gradients (β). Predictions by the standard k–ε model give some higher dp/dx values than the data of ref. [18] and Hong *et al.*'s [19] semi-empirical predictions. However, predictions by the present curvature correction model agree well with refs. [18, 19] except near $P/H = 5$ for $Re = 30\,000$. For $Re = 39\,000$, we cannot obtain any conclusions from the comparison of predictions with experimental data since the data is only one.

Figure 9 shows the variation of the mean dimensionless axial velocity ($\bar{U}^+$) with respect to y^+. The mean axial velocity $\bar{U}_j$ at an arbitrary grid line j was calculated by averaging the predicted local velocity U_{ij} in the x-direction from the inlet grid line to the outlet grid line as follows:

$$\bar{U}_j = \frac{\sum_{i=1}^{n} U_{ij}\Delta x_i}{\sum_{i=1}^{n} \Delta x_i} \tag{24}$$

where Δx_i is the width of the ith grid in the axial direction and $\Sigma_{i=1}^{n} \Delta x_i$ is the length of one pitch of roughness. Then $\bar{U}_j^+$ can be calculated by non-dimensionalizing $\bar{U}_j$ by the friction velocity $\sqrt{(\tau_{w1}/\rho)}$ where τ_{w1} is the mean wall shear stress of the inner wall. This can be calculated if the mean axial pressure gradient (β) and mean wall shear stress of the outer wall (τ_{w2}) were predicted. It is interesting that the $\bar{U}^+$ profile for $P/H = 3$ is different from the profiles for other values of P/H. This is due to the fact that for $P/H = 3$ the separated flow by rib cannot be reattached to the inner wall and the cavity flow is generated between the ribs. It is a difficult problem to calculate the function R accurately from the $\bar{U}^+$ profile, since generally $\bar{U}^+$ profiles for $y^+ > h^+$ are not straight lines as shown in Fig. 10.

In this study, the function R was calculated by the following method. First, the straight line with gradient $1/\kappa$ was contacted with curve AB in Fig. 10. The intercept of this straight line with the line $y^+ = h^+$ was taken as R_1. Next, the straight line parallel to this line was drawn passing through point A. The value of $\bar{U}^+$ for point A was taken as R_2. Then the representative straight line for curve AB would be located between these two lines. Using this method we determined R as the average of R_1 and R_2.

Figure 11 shows the comparison of the function R predicted by the present method with Dalle Donne and Meyer and Han *et al.*'s correlation. Data on Fig. 11 were taken from Fig. 38 and Table 2 of ref. [5]. These are a collection of data from many works. The

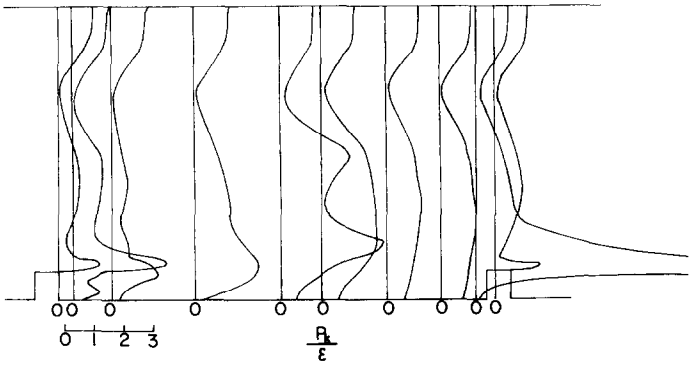

FIG. 7. Ratio of the production rate to the dissipation rate of turbulent kinetic energy for $Re = 30\,000$ and $P/H = 15$.

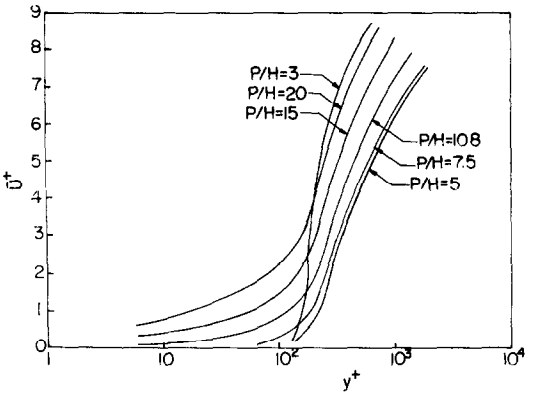

FIG. 9. Predicted mean dimensionless axial velocity with respect to y^+ by present curvature correction model for $Re = 30000$.

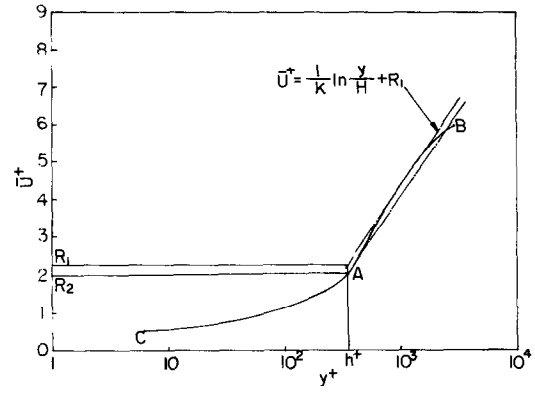

FIG. 10. Schematic of determination of R function from $\bar{U}^+$ profile.

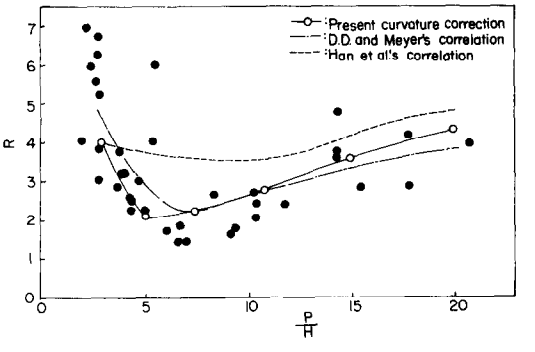

FIG. 11. Comparison of predicted R function by present method with previous correlations; ●, data taken from ref. [5].

predicted R function has lower values than Han *et al.*'s correlation but has a similar profile to that of Dalle Donne and Meyer's correlation which is known to be the most accurate correlation. This fact suggests the possibility of a theoretically accurate prediction of the R function.

Figure 12 shows the periodic temperature profiles of air for $Re = 30000$ and $P/H = 5$. Both predictions by the standard k–ε model and curvature correction model agree well with Kang's [16] experimental data

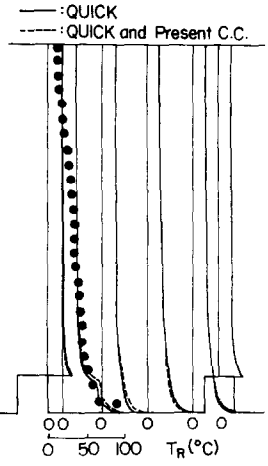

FIG. 12. Periodic temperature distribution of air for $Re = 30000$ and $P/H = 5$. Data taken from Kang [16].

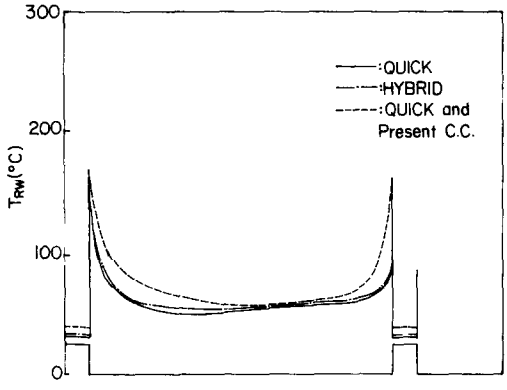

FIG. 13. Periodic wall temperature distribution of inner wall with roughness for $Re = 30000$ and $P/H = 10.8$.

near the inner wall, however, approaching the outer wall the difference becomes larger. This is due to the fact that in Kang's experiment the outer pipe was not insulated where the air temperatures were measured.

Figure 13 shows the wall temperature distribution of the inner wall with roughness. Predictions by the QUICK and HYBRID schemes at the standard k–ε model give similar profiles. However, the prediction by the present curvature correction shows a different profile from those by the standard k–ε model, especially at the wall attached to the recirculation region.

Figure 14 shows the comparison of predicted local Nusselt numbers of the inner wall. Local Nusselt numbers have maximum values near the reattachment point of the separated flow by roughness. The present curvature correction model gave Nusselt number distributions different from those by standard k–ε model.

Figure 15 shows the comparison of the mean Nusselt numbers of the inner wall obtained by averaging the local Nusselt numbers in the x-direction. All the present predictions give lower values than Kang's data. This may be due to the inappropriate correlation of the turbulent Prandtl number in this analysis. In

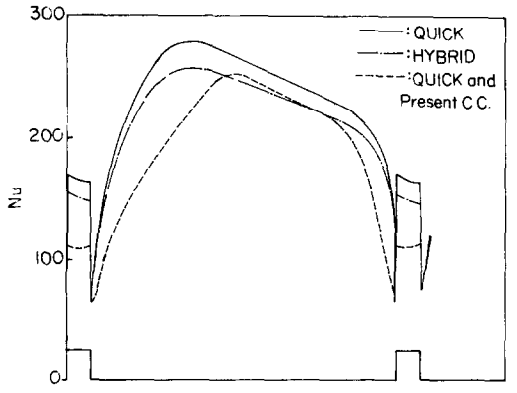

FIG. 14. Local Nusselt number of inner wall for $Re = 30\,000$ and $P/H = 10.8$.

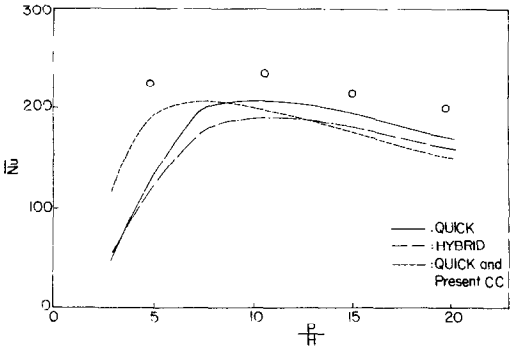

FIG. 15. Mean Nusselt number of inner wall for $Re = 30\,000$. Data taken from Kang [16].

this analysis following Crawford and Kays' correlation [25] for the turbulent Prandtl number

$$Pr_t = \left(\frac{\alpha^2}{2} + 0.2\alpha\, Pe_t - (0.2Pe_t)^2 \times (1.0 - \exp(-\alpha/(0.2Pe_t))\right)^{-1}$$

where

$$Pe_t = (\nu_t/\nu)Pr, \alpha = \sqrt{(1/Pr_{t,ref})}, Pr_{t,ref} = 0.86. \quad (25)$$

However, Fig. 15 shows that the shape of the $\overline{Nu}$ profile predicted by the present curvature correction model is better than those by the standard k–ε model. In order to obtain a more accurate Nusselt number profile, more profound studies on the turbulent Prandtl number model in the recirculation flow is necessary.

Figure 16 shows a comparison of the present prediction of the G function with previous correlations. In previous correlations $h^+ (= h\sqrt{(\tau_{w1}/\rho)}/\nu)$ was calculated from the predicted mean shear stress of the rough wall, τ_{w1}. For P/H between 5 and 17.5, the predicted G function lies between Dalle Donne and Meyer and Han *et al.*'s correlation. However, for a P/H less than 5 and greater than 17.5, predictions have larger values than these correlations. In most of

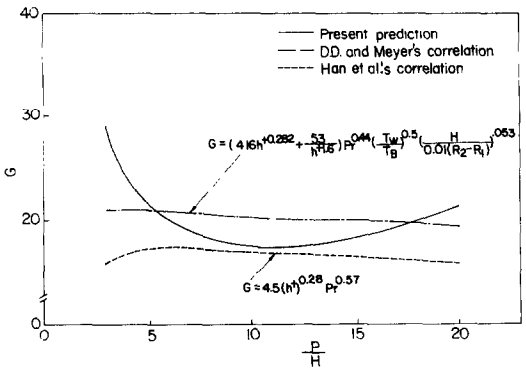

FIG. 16. Comparison of predicted G function with previous correlations for $Re = 30\,000$.

the previous studies, G functions were not correlated by the function of P/H. However, the present prediction shows that the G function is clearly the explicit function of P/H. Since present analyses were performed with only the variation of P/H and Reynolds number, in order to prove the compatibility of the present transformation method, more computations with a variation of boundary conditions and flow conditions are necessary.

5. CONCLUSIONS

Generalized concepts of periodic fully developed turbulent flow and heat transfer have been formulated for the analysis of an annular pipe with rectangular roughness under fully developed conditions. The velocity components are periodic and pressure can be reduced to a periodic function after subtraction of a linear term relates to the global through flow. Two discretization schemes at the standard k–ε model and modified streamline curvature correction model have been applied to the analysis and their performances have been examined. Roughness functions related to the velocity and temperature profiles have been calculated theoretically from numerically predicted mean dimensionless velocity and temperature profiles. These studies allow the following conclusions.

(1) QUICK and HYBRID schemes give nearly the same velocity profiles in the region where streamlines are nearly parallel to grid lines, however, in the region where streamlines cross grid lines with inclined angles they show different profiles.

(2) More improved predictions of velocity profiles and mean pressure gradients can be obtained by applying the modified streamline curvature correction model rather than by the standard k–ε model.

(3) Predicted roughness functions agree reasonably with previous correlations. This implies the possibility of accurate predictions of roughness functions.

(4) Prediction shows that the G function is the explicit function of P/H contrary to the correlations in the previous studies.

Acknowledgement—The authors wish to express their gratitude to KOSEF for their financial support during 1982–1983. They would also like to thank Miss Kim for her expert typing of the manuscript.

REFERENCES

1. W. B. Hall, Heat transfer in channels having rough and smooth surfaces, *J. Mech. Engng Sci.* **4**(3), 281–291 (1962).
2. D. Wilkie, Calculation of heat transfer and flow resistance of rough and smooth surfaces contained in a single passage, E.A.E.S. Heat Transfer Symp. on Superheated Stream or Gas, Berne, Switzerland, Sept. (1966).
3. K. Maubach, Rough annulus pressure drop. Interpretation of experiments and recalculation for square ribs, *Int. J. Heat Mass Transfer* **15,** 2489–2498 (1972).
4. M. Dalle Donne and E. Meerwald, Heat transfer and friction coefficients for turbulent flow of air in smooth annuli at high temperature, *Int. J. Heat Mass Transfer* **16,** 787–809 (1973).
5. M. Dalle Donne and L. Meyer, Turbulent convective heat transfer from rough surfaces with two dimensional rectangular ribs, *Int. J. Heat Mass Transfer* **20,** 583–620 (1977).
6. J. C. Han, L. R. Glicksman and W. M. Rohsenow, An investigation of heat transfer and friction for rib roughened surfaces, *Int. J. Heat Mass Transfer* **21,** 1143–1156 (1978).
7. D. F. Dipprey and R. H. Sabersky, Heat and momentum transfer in smooth and rough tubes at various Prandtl number, *Int. J. Heat Mass Transfer* **6,** 329–353 (1963).
8. P. Bradshaw, Effects of streamline curvature on turbulent flows, *AGARDograph* 169 (1973).
9. B. E. Launder, C. H. Priddin and B. S. Sharma, The calculation of turbulent boundary layers on spinning and curved surfaces, *Trans. ASME J. Fluids Engng* **99,** 231–239 (1977).
10. W. Rodi, Influence of buoyancy and rotation on equations for the turbulence length scale, *Proc. 2nd Symp. on Turbulent Shear Flows*, Imperial College, London, pp. 10.37–10.42 (1979).
11. M. A. Leschziner and W. Rodi, Calculation of annular and twin parallel jets using various discretization schemes and turbulence model variations, *Trans. ASME J. Fluids Engng* **103,** 352–360 (1981).
12. B. E. Launder, Private communication (1984).
13. S. V. Patankar, C. Liu and E. M. Sparrow, Fully developed flow and heat transfer in ducts having streamwise-periodic variations of cross-sectional area, *Trans. ASME J. Heat Transfer* **99,** 180–186 (1977).
14. B. E. Launder, A. P. Morse, W. Rodi and D. B. Spalding, Prediction of free shear flows—a comparison of performance of six turbulence model, *Proc. Largley Free Shear Flows Conf.*, NASA Rep. SP 320, 361 (1973).
15. K. Hanjalic and B. E. Launder, Sensitizing the dissipation equation to irrotational strains, *Trans. ASME J. Fluids Engng* **102,** 34–40 (1980).
16. J. S. Kang, Experiment of turbulent heat transfer on the annular pipes with ring and spiral artificial roughness, Master's Thesis, Korea University (1983).
17. J. S. Kang and Y. D. Choi, Study on the effects of artificial roughness on the turbulent heat transfer of concentric annular pipes, *J. KSME* **9**(3), 335–344 (1985).
18. K. M. Lee, The experiment of turbulent heat transfer in annular pipe with artificial roughness, Master's Thesis, Korea University (1982).
19. J. K. Hong, K. M. Lee and Y. D. Choi, Analysis of turbulent heat transfer in a concentric annular pipe with artificial roughness, *J. KSME* **7**(3), 301–312 (1983).
20. R. Aris, *Vectors, Tensors and the Basis Equations of Fluid Mechanics*. Prentice-Hall, Englewood Cliffs, New Jersey (1962).
21. R. W. Johnson, Turbulent convecting flow in a square duct with a 180° bend; an experimental and numerical study, Ph.D. Thesis, UMIST, pp. 216–219 (1984).
22. S. V. Patankar, *Numerical Heat Transfer and Fluid Flow*, pp. 131–134. McGraw-Hill, New York (1980).
23. D. P. Leonard, A stable and accurate convective modelling procedure based on quadratic upstream interpolation, *Comput. Meth. Appl. Mech. Engng* **19,** 59–98 (1979).
24. S. V. Patankar and C. Prakash, An analysis of the effect of plate thickness on laminar flow and heat transfer in interrupted plate passage, *Int. J. Heat Mass Transfer* **24,** 1801–1810 (1981).
25. M. E. Crawford and W. M. Kays, STAN5—a program for numerical computation of two dimensional internal/external boundary layer flows, Report HMT-23, Stanford University (1975).

ECOULEMENT TURBULENT PERIODIQUEMENT PLEINEMENT ETABLI ET TRANSFERT THERMIQUE ANALYSES PAR UN MODELE k–ε DANS UN ESPACE ANNULAIRE ARTIFICIELLEMENT RUGUEUX

Résumé—On analyse à l'aide d'un modèle k–ε les écoulements turbulents périodiquement établis, avec transfert de chaleur à partir d'un cylindre intérieur à un espace annulaire artificiellement rugueux. Un nouveau modèle de correction de courbure de ligne de courant pour la viscosité turbulente et un TDMA cyclique sont appliqués de façon à augmenter la précision et la vitesse de convergence des solutions numériques. On illustre la nouvelle méthode d'obtention des fonctions de rugosité à partir des profils de vitesse et de température calculés. Une fonction de rugosité liée au profil de vitesse s'accorde bien avec des corrélations semi-empiriques déjà connues, mais une autre pour le profil de température montre une forme qui diffère d'autres proposées antérieurement.

UNTERSUCHUNG EINER PERIODISCH VOLLAUSGEBILDETEN TURBULENTEN STRÖMUNG UND DES WÄRMEÜBERGANGS IN KÜNSTLICH AUFGERAUHTEN RINGSPALTEN MIT DEM k–ε-GLEICHUNGS-MODELL

Zusammenfassung—Es werden periodisch voll ausgebildete turbulente Strömungen mit Wärmeübergang am inneren Rohr eines künstlich aufgerauhten Ringspaltes mit Hilfe des k–ε-Gleichungs-Modells untersucht. Ein neues Modell (mit Korrektur der Stromlinien-Krümmung) für die Scheinviskosität und die zyklische TDMA wird angewandt, um die Genauigkeit und die Konvergenzrate der numerischen Lösungen zu erhöhen. Diese Arbeit legt die neue Methode dar, Rauhigkeitsfunktionen aus numerisch ermittelten Geschwindigkeits- und Temperaturprofilen zu bestimmen. Die ermittelte Rauhigkeitsfunktion bezüglich des Geschwindigkeitsprofils stimmt gut mit früheren halbempirischen Korrelationen überein, aber die Rauhigkeitsfunktion für das Temperaturprofil weicht vom Verlauf früherer Funktionen ab.

АНАЛИЗ ПЕРИОДИЧЕСКИ НЕСТАЦИОНАРНОГО ПОЛНОСТЬЮ РАЗВИТОГО ТУРБУЛЕНТНОГО ТЕЧЕНИЯ И ТЕПЛОПЕРЕНОСА В КОЛЬЦЕВОМ КАНАЛЕ С ИСКУССТВЕННОЙ ШЕРОХОВАТОСТЬЮ С ПОМОЩЬЮ k–ε МОДЕЛИ

Аннотация—С помощью k–ε модели проанализированы периодически полностью развитые турбулентные течения в кольцевом канале с теплопереносом от внутренней трубы при наличии искусственной шероховатости. Для повышения точности и сходимости численных решений предложены новые зависимости турбулентной вязкости и температуропроводности от кривизны линий тока. Предложен новый метод получения функций шероховатости, основанный на численном эксперименте; полученная таким образом функция шероховатости, относящаяся к скорости, хорошо согласуется с ранее полученными полуэмпирическими зависимостями, в то время как соответствующая функция для профиля температуры отличается от ранее предложенных.